For the example shown in Fig. 1, the incorporation of BME-44 as potassium carrier gives a potential shift of 324 mV, suggesting that the uncomplexed potassium concentration is decreased by a factor of 3.5×10^5, which translates into an effective stability constant $\log \beta_{KL} = 7.8$. The data from Fig. 2 reveal the complexation of sodium ions by the carrier. The observed potential shift of 159 mV can be related to an effective complex formation constant of $\log \beta_{NaL} = 5.0$. These data correspond well to the ones obtained previously with optical measurements on thin polymeric films coated on glass slides, 7.9 and 5.5 respectively.[4] This suggests that the transition from optical to potentiometric measurements may be a valid approach to the characterization of neutral cation carriers. Since the electrode response in the activity region of cation interference should be fully governed by the incorporated potassium carrier, the potential differences between potassium and sodium response should be comparable to the potassium selectivity of established potentiometric sensors containing this ionophore. The data presented here suggest a Nicolskii coefficient of $\log K^{pot}_{KNa} = -3.2$, which is comparable to values reported earlier.[11] Interestingly, the difference in the two logarithmic complex formation constants as obtained in this work is only −2.8. This again confirms that the selectivity of ion-selective electrodes is not only given by the ratio of complex formation constants but also by the relative lipophilicities of the ions. At high sample pH, the measured potentials of membranes with H^+ ionophore only are 24 mV lower in sodium chloride solutions than in potassium chloride (see Fig. 1 and 2). Since potassium ions are somewhat more lipophilic, the potassium selectivity of the sensor is higher than expected on the basis of complex formation alone. This example shows how the addition of a second ionophore to the membrane can reveal these processes in an elegant way.

Conclusions

Since ion-selective electrode membranes respond to the activity ratio of uncomplexed ions in the membrane and aqueous phase, they are in principle appropriate experimental tools to assess complex formation constants of ion carriers directly within the membrane phase. The experimental drawbacks that the complex formation occurs simultaneously at the membrane-inner filling solution and that the electrode response is also dependent on the relative lipophilicity of the extracted ion however has prohibited such an approach in the past. We have circumvented these problems by proposing to incorporate an additional, highly selective H^+ carrier into the membrane that allows for the direct measurement of effective complex formation constants of ionophore complexes within solvent polymeric membranes. Further studies in this direction are in progress.

Acknowledgment

The authors thank Auburn University, Hitachi Ltd., and Orion Research Inc. for financial support.

Manuscript submitted Dec. 9, 1996; revised manuscript received Feb. 5, 1997.

Auburn University assisted in meeting the publication costs of this article.

REFERENCES

1. R. Bliggensdorfer, G. Suter, and W. Simon, *Helv. Chim. Acta,* **72,** 1164 (1989).
2. E. Eyal and G. A. Rechnitz, *Anal. Chem.*, **43,** 1090 (1971).
3. W. E. Morf, *The Principles of Ion-Selective Electrodes and of Membrane Transport,* Elsevier, New York (1981).
4. E. Bakker, M. Willer, M. Lerchi, K. Seiler, and E. Pretsch, *Anal. Chem.*, **66,** 516 (1994).
5. M. Erdosy, E. Lindner, and R. P. Buck, In preparation.
6. E. Bakker, M. Lerchi, T. Rosatzin, B. Rusterholz, and W. Simon, *Anal. Chim. Acta,* **278,** 211 (1993).
7. M. Nägele and E. Pretsch, *Mikrochim. Acta,* **121,** 269 (1995).
8. E. Bakker, A. Xu, and E. Pretsch, *Anal. Chim. Acta.*, **295,** 253 (1994).
9. E. Bakker, M. Nägele, U. Schaller, and E. Pretsch, *Electroanalysis,* **7,** 817 (1995).
10. R. D. Armstrong and G. Horvai, *Electrochim. Acta,* **35,** 1 (1990).
11. E. Lindner, I. Bitter, B. Agai, E. Pungor, K. Toth, L. Toke, M. Horvath, and Z. Hell, *Fres. Z. Anal. Chem.*, **322,** 157 (1985).

Self-Ordering of Cell Arrangement of Anodic Porous Alumina Formed in Sulfuric Acid Solution

Hideki Masuda and Fumio Hasegwa

Department of Industrial Chemistry, Faculty of Engineering, Tokyo Metropolitan University, 1-1 Minamiosawa, Hachioji, Tokyo 192-03, Japan

Sachiko Ono*

Advanced Research Institute for Science and Engineering, Waseda University, 3 Ohkubo, Shinjuku-ku, Tokyo 169, Japan

ABSTRACT

Self-ordering of the cell arrangement of the porous structure of anodic alumina has been studied in a sulfuric acid solution. Ordering of the cell arrangement was dependent on the applied potential, and a highly ordered structure was obtained under anodization at a constant potential of 25 to 27 V. Self-ordering of the porous structure proceeded with the growth of the oxide layer under anodization at an appropriate potential, and a porous film with an almost ideal hexagonal honeycomb structure was formed over an area of several micrometers after a long period of anodization.

Introduction

Anodic porous alumina, which has a typical naturally occurring self-ordered structure, has recently attracted increasing attention as a key material for fabrication of devices on a nanometer scale, such as electronic and photoelectronic devices,[1-9] and for application to micro- and ultrafiltration.[10-13] For these applications, well-characterized regular membranes with ideal pore configurations are particularly useful.

The geometry of anodic porous alumina may be schematically represented as a honeycomb structure which is characterized by a close-packed array of columnar hexagonal cells, each containing a central pore normal to the substrate, as shown in Fig. 1.[14,15] However, the geometry of the anodic porous alumina usually obtained is far from the idealized model; that is, the cells are irregular polygons, and the arrangement of the cells and pores is not ideal hexagonal. This irregularity of the porous structure causes distortion of the cross section of the pores and broadening of the pore diameter distribution.

Recently we reported that a highly ordered honeycomb structure with an almost ideal hexagonal arrangement can be obtained over relatively large areas under a specific anodizing condition in oxalic acid solution.[16-18] The condition of the self-ordering of the cell arrangement was characterized by a longer anodization period compared to the usual anodizing and application of a constant appropriate anodizing potential. The most appropriate potential for the ordering of the cell arrangement in oxalic acid was *ca.* 40 V, and at a lower anodizing potential, *e.g.,* 25 V, ordering could not be observed.

This new type of anodic porous alumina with an ideal regular structure can be used for many applications. The long-range ordering of anodic porous alumina is advantageous to optimize the

* Electrochemical Society Active Member.

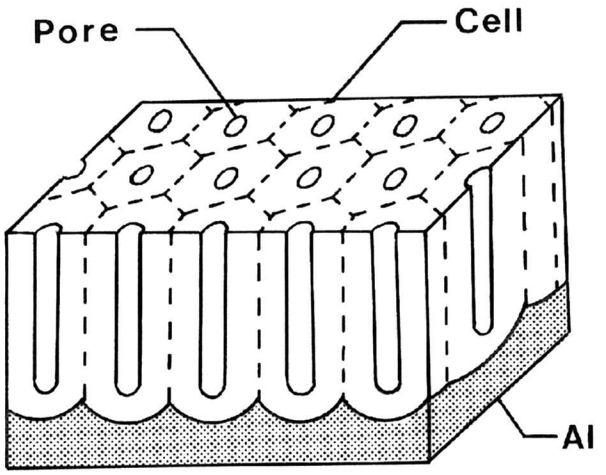

Fig. 1. Schematic model of ideal porous structure of anodic alumina.

properties of the fabricated devices. In addition to this, an ideally arranged hexagonal configuration of the cells contributes to a narrowing of the size distribution of pores because of their almost perfect circular section. Furthermore, there has been strong interest in fundamental studies of the self-ordering on a nanometer scale of such oxide films on metals.

In this article we show that the ordered structure can be obtained in a sulfuric acid solution,[19] which is the solution most commonly used to anodize Al. The ordering of the cell arrangement of the film occurred under a constant potential condition in a similar manner to anodization in oxalic acid. However, the potential required for self-ordering evidently differs from that required in oxalic acid. This finding is of great practical importance in extending the range of anodizing conditions for the highly ordered structure, because the cell size is known to be directly related to the anodizing potential.[15]

Experimental

An aluminum sheet (99.99% purity, 10 × 50 × 0.3 mm) was degreased in acetone, and was electropolished under a constant-current condition of 100 mA cm^{-2} for 3 min in a mixed solution of $HClO_4$ and C_2H_5OH.

Anodizing was conducted under a constant cell potential condition in a sulfuric acid solution. It can be expected that ordering of the cell arrangement occurs under the long-period anodization at an appropriate potential. For this reason, the cell configuration was examined by changing the applied potential and anodizing period.

After anodization, the anodic oxide film was chemically removed from the aluminum using a saturated Hg_2Cl_2 solution. Subsequent etching treatment was carried out in a 5 weight percent (w/o) H_3PO_4 solution at 30°C. This makes it easy to observe the arrangement of the pores by removing the bottom part of the anodic oxide film called the barrier layer. The structures of the anodic porous alumina formed under different conditions were observed from the bottom side of the film using a scanning electron microscope (SEM, JEOL JSM-6100).

Results and Discussion

At the initial stage of anodization of aluminum, the points of pore initiation are spread randomly over the aluminum surface.[15] Ordering of the cell arrangement proceeds with the anodizing time after steady state in the growth of the porous structure is established. Therefore, the ordered structure cannot be observed at the surface of the film. We examined the cell arrangement of the film from the bottom side of the membrane after removing the Al substrate with an etching treatment in a saturated Hg_2Cl_2 solution and subsequent removal of the barrier layer in an H_3PO_4 solution.

SEM micrographs of the cell arrangement obtained different anodizing potential are shown in Fig. 2. Observation of the cell arrangement was carried out using films with an almost constant thickness of 25 ± 3 μm, because the ordering of the cell arrangement was dependent on the film thickness. As clearly shown in Fig. 2, the ordering of the cell arrangement was dependent on the anodizing potential. The most appropriate potential for cell ordering was 25 to 27 V. Because stable anodizing at potential above 27 V was difficult to maintain due to the occurrence of pitting on the surface, we could not examine the dependence of the ordering on anodizing potential above 27 V. Self-ordering of the cell arrangement could not be observed at 25 to 27 V in oxalic acid solution. This result indicates that self-ordering, which controls the cell arrangement, occurs only in the specified potential region, and the most appropriate potential for self-ordering varies according to the anodization solution.

Figure 3 shows the dependence of the regularity of the cell arrangement on the thickness of the film obtained at an anodizing potential of 25 V. Other parameters in anodizing, such as concentration of the sulfuric acid and temperature of the solution, did not clearly affect the self-ordering of the cell arrangement. In Fig. 3, the time required to form the films is described along with the thick-

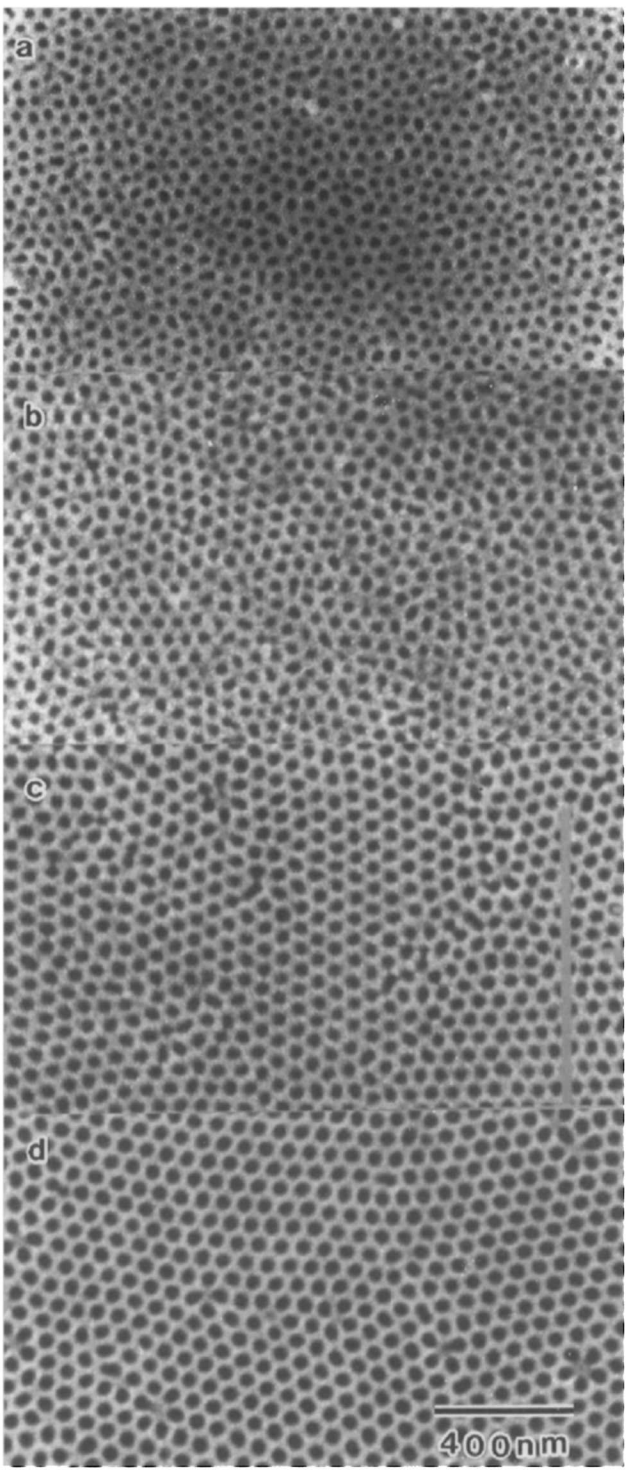

Fig. 2. SEM micrographs of anodic porous alumina formed under different potential conditions, in 0.3 *M* H_2SO_4 solution at 0°C; (a) 20, (b) 23, (c) 25, and (d) 27 V. Anodizing periods are: (a) 1500, (b) 1000, (c) 706, and (d) 450 min.

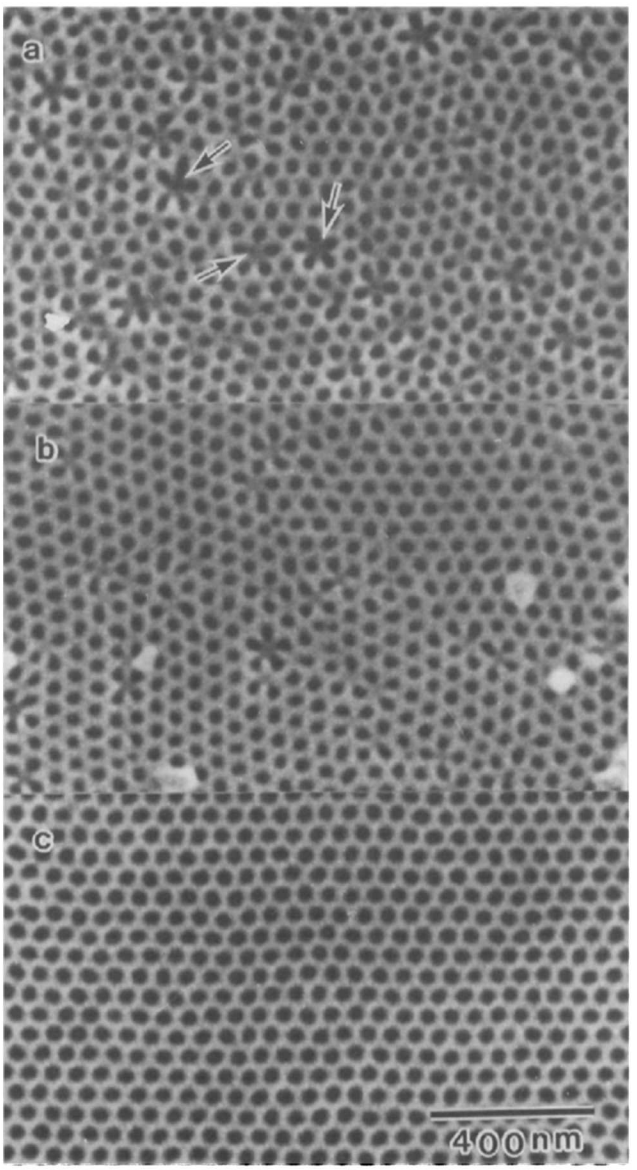

Fig. 3. Dependence of ordering of the cell arrangement of anodic porous alumina on the thickness of the film, obtained in 0.5 *M* H_2SO_4 at 25 V and 10°C; (a) 2.4 μm [9 min], (b) 10.6 μm [36 min], and (c) 202 μm [750 min].

ness. It is shown that self-ordering proceeds with the growth of the oxide film and that a porous structure with an almost ideal hexagonal structure was obtained over an area of several micrometers after anodization for 750 min.

In the porous structure, characteristic patterns of pore configurations can be observed, as indicated by the arrows in Fig. 3a. Most pores are arranged in a hexagonal configuration with an almost perfectly round section, while the characteristic patterns at defects were composed of distorted circular pores. With ordering of the cell configuration, the number of occurrences of these patterns decreases, and an improved ordered structure is formed.

From the low-magnification micrograph in Fig. 4, it is seen that the part with an ideal cell arrangement has a domain structure, on the boundary of which defects are concentrated. These cell arrangements are similar to those obtained using an oxalic acid solution except that the potential required for ordering in the sulfuric acid differs from that required in oxalic acid.[17]

The detailed mechanism of formation of the highly ordered structure is not yet clear. During the steady-state growth of films under constant-potential conditions, cells with almost identical size must generate a regular arrangement of close-packed arrays of hexagonal cylinders. However, under the usual anodizing conditions, perturbations in the configuration of the grown cells result in a large number of defects in the cell arrangement. It is assumed that during anodization at a specific potential, almost perturbationless growth becomes feasible resulting in a highly ordered structure.

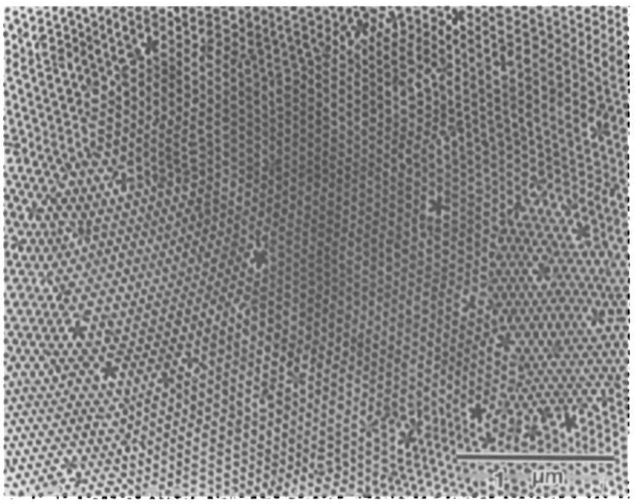

Fig. 4. Low-magnification SEM micrograph of the film. The anodizing conditions are the same as those for Fig. 3c.

Conclusion

Anodic porous alumina with an almost ideal ordered honeycomb structure could be obtained in sulfuric acid solution. The potential required for self-ordering was lower than that for oxalic acid solution, which permits fabrication of an ordered structure with smaller dimensions.

In the anodization procedure used here, an ordered structure could be formed only at the bottom of the film. For the fabrication of the symmetrical films with straight holes throughout the entire film, a two-step anodization process[18] can be used. In this process, the concave texture of the Al surface which is formed by selective removal of the film after the first anodizing step can induce ordered formation of pores even at the initial stage of anodization in the second anodizing step.

In previous reports, we demonstrated the preparation of nanohole arrays of metals[17,20,21] and semiconductors,[22-24] using two-step replication of the honeycomb structure of the anodic porous alumina prepared in oxalic acid solution. The ordered anodic porous alumina obtained in the sulfuric acid solution can be used to fabricate nanohole arrays with finer dimensions than those obtained in the oxalic acid solution.

Acknowledgment

This work was partially supported by a Grant-in Aid on Priority Area Research (No. 282) from the Ministry of Education, Science, and Culture, Japan.

Manuscript submitted Nov. 8, 1996; revised manuscript received Jan. 24, 1997.

Tokyo Metropolitan University assisted in meeting the publication costs of this article.

REFERENCES

1. C. A. Huber, T. E. Huber, M. Sadoqi, J. A. Lubin, S. Manalis, and C. B. Prater, *Science,* **263,** 800 (1994).
2. S. Kawai and R. Ueda, *This Journal,* **122,** 32 (1975).
3. T-J. Cheng, J. Jorne, and J.-S. Gau, *ibid.,* **137,** 93 (1990).
4. C. G. Granqvist, A. Anderson, and O. Hunderi, *Appl. Phys. Lett.,* **35,** 268 (1979).
5. D. G. W. Goad and M. Moskovits, *J. Appl. Phys.,* **49,** 2929 (1978).
6. C. K. Preston and M. Moskovits, *J. Phys. Chem.,* **92,** 2957 (1988).
7. M. Saito, M. Kirihara, T. Taniguchi, and M. Miyagi, *Appl. Phys. Lett.,* **55,** 607 (1989).
8. M. J. Tierney and C. R. Martin, *J. Phys. Chem.,* **93,** 2878 (1989).
9. I. Mizuki, H. Masuda, and N. Baba, in *Proceedings of the Third Symposium of the IUMRS International Conference, Advanced Materials,* Vol. 15A, p. 381 (1994).
10. K. Itaya, S. Sugawara, K. Arai, and S. Saito, *J. Chem. Eng. Jpn.,* **17,** 514 (1984).
11. R. C. Furneaux, W. R. Righy, and A. P. Davidson, *Nature,* **337,** 147 (1989).
12. S. E. Jones, S. A. Ditner, C. Freeman, C. J. Whitaker, and M. A. Lock, *Appl. Environ. Microbiol.* **55,** 529 (1989).
13. S. K. Dalvie and R. E. Baltus, *J. Membr. Sci.,* **71,** 247 (1992).

14. F. Keller, M. Hunter, and D. L. Robinson, *This Journal*, **100**, 411 (1953).
15. J. P. O'Sullivan and G. C. Wood, *Proc. R. Soc. London, Ser. A*, **317**, 511 (1970).
16. H. Masuda, Y. Nakayama, K. Fukuda, and N. Baba, Abstract of 89th Meeting of Surf. Fin. Soc. Jpn., p. 107, Yokohama, Tokyo (1994).
17. H. Masuda and K. Fukuda, *Science*, **268**, 1466 (1995).
18. H. Masuda and M. Satoh, *Jpn. J. Appl. Phys.*, **35**, L126 (1996).
19. F. Hasegawa, S. Ono, and H. Masuda, Abstract of 93rd Meeting of Surf. Fin. Soc. Jpn., p. 267, Chiba, Japan (1996).
20. H. Masuda, H. Tanaka, and N. Baba, *Chem. Lett.*, 621 (1990).
21. H. Masuda, K. Nishio, and N. Baba, *Thin Solid Films*, **223**, 1 (1993).
22. H. Masuda, K. Nishio, and N. Baba, *Jpn. J. Appl. Phys.*, **31**, L1775 (1992).
23. P. Hoyer, N. Baba, and H. Masuda, *Appl. Phys. Lett.*, **66**, 2700 (1995).
24. P. Hoyer and H. Masuda, *J. Mater. Sci. Lett.*, **15**, 1228 (1996).

Low-Temperature Solid-Oxide Fuel Cells Utilizing Thin Bilayer Electrolytes

Tsepin Tsai,* Erica Perry, and Scott Barnett

Department of Materials Science and Engineering, Northwestern University, Evanston, Illinois 60208, USA

ABSTRACT

Solid-oxide fuel cells (SOFCs) with electrolytes that provide high open-circuit voltage (OCV) and low ohmic loss down to 550°C are described. The electrolytes were bilayers consisting of a 4 to 8 μm thick Y-doped ceria (YDC) layer with a 1 to 1.5 μm thick Y-doped zirconia (YSZ) layer on the fuel side. The cathode/supports were $La_{0.85}Sr_{0.15}MnO_3$-YSZ. The anodes consisted of thin YDC and Ni-YSZ layers. The YDC/YSZ electrolyte SOFCs yielded 85 to 98% of the theoretical OCV, compared with ≈50% for YDC electrolyte SOFCs. The cathode overpotential, which was a main factor limiting SOFC power density, was lower for YDC/YSZ than YSZ electrolytes. The maximum power density at 600°C, 210 mW/cm², is higher than for previously reported SOFCs.

Introduction

Lowering SOFC operating temperatures T_c below ≈1000°C is of interest for allowing the use of higher performance, lower cost materials for the stack and balance-of-plant, reducing stack thermal-insulation requirements, and increasing cell life because of reduced thermal degradation and thermal cycling stress.[1] Recent advances have led to SOFCs yielding high power densities at T_c down to 700°C.[1-4] Achieving T_c values from ≈450 to 650°C would be particularly useful for two main reasons. First, low cost ferritic stainless steels, that retain significant strength in this temperature range, could be used for stack components, such as interconnects and gas manifolds. Second, there are indications that direct oxidation of methane without carbon deposition is possible at ≤650°C,[5] eliminating the need for fuel reforming. However, there are significant barriers to low-temperature (450 to 650°C) SOFCs: electrolyte ohmic resistance and electrode overpotentials.

In most medium temperature (700 to 800°C) SOFCs, an ≈10μm thick YSZ electrolyte is employed to minimize ohmic loss.[1-4] However, the YSZ area-specific resistance for a 10 μm thickness becomes appreciable at 600°C, ≈0.5 Ω cm², and is very large at 500°C, ≈2 Ω cm². While significantly thinner YSZ electrolytes would allow lower T_c, the long-term stability and reliability of very thin electrolytes remains an issue. Thus, oxide materials with higher conductivity σ should be considered. However, they typically have some property that precludes their use in SOFCs; doped $BaCeO_3$ appears to exhibit mixed conductivity,[6] while doped Bi_2O_3 is reduced by typical fuel gases and Sc-doped ZrO_2 undergoes a structural transformation at ≈600°C.[7] A relatively new candidate, (La,Sr)(Ga,Mg)O (LSGM), appears promising.[8] Much of the work on alternate electrolytes has focused on ceria.[9-16] Representative σ values for Sm, Gd, or Y-doped ceria[11] are ≈3 times that for YSZ, such that ohmic losses with ≈10 μm thick ceria electrolytes would extend the range of SOFC operation to well below 600°C. The electronic conductivity and volume change observed on reduction of ceria are serious problems. For example, an anode-supported SOFC with a 5 to 10 μm thick Gd-doped ceria (GDC) electrolyte provided an OCV value <70% of theoretical, along with a low maximum power density of ≈70 W/cm², at 600°C.[9] While the electrolytic domain increases with decreasing T_c, the electronic conductivity of GDC is negligible only for $T_c \leq 450$°C.[12] Other dopants, *e.g.*, Sm [11] or Gd-Pr double doping,[9,13] may slightly increase the electrolytic domain compared to Gd, but not enough for typical SOFC fuel gases at $T_c > 450$°C. One method for obtaining high OCV with ceria electrolytes is to add a YSZ layer to block the electronic current.[14,15]

SOFC overpotentials typically increase rapidly for T_c decreased below 700°C,[2] limiting power densities. The electrolyte material chosen should help minimize overpotentials. Oxygen surface exchange coefficients are higher for ceria than any other electrolyte materials for which data are available, suggesting that it would provide optimal cathode performance.[16] Y-doped ceria (YDC) interfacial layers have been shown to decrease anode overpotentials.[17]

In this article, we describe results on SOFCs with bilayer yttria-doped ceria (YDC)/YSZ electrolytes that provide low electrolyte ohmic loss, decrease overpotentials, and overcome the problems associated with reduction of ceria. The maximum power density of 210 mW/cm² at 600°C compares favorably with the highest value that has been reported for a SOFC at this temperature, ≈140 mW/cm².[9]

Experimental

The cells were deposited on $La_{0.85}Sr_{0.15}MnO_3$-YSZ support/cathodes that were prepared using ceramic processes.[2] $(Y_2O_3)_{0.15}(CeO_2)_{0.85}$(YDC) and $(Y_2O_3)_{0.1}(ZrO_2)_{0.9}$ (YSZ) were reactively sputter deposited at ≈5 μm/h from Y-Ce and Y-Zr composite targets, respectively, in Ar-O_2 mixtures (1 to 1.2 Pa Ar, ≈0.013 Pa O_2). The substrate temperature was ≈400°C, and a negative substrate bias V_s was used throughout electrolyte deposition. Previous studies of YSZ deposition showed that V_s = 75 V produced high-density films.[18] However, larger V_s values led to delamination of the electrolyte from the cathode due to compressive film stress. Two types of electrolytes were prepared. One was an 8 μm thick YDC layer followed by a 1 μm thick YSZ layer (8YDC/1YSZ) deposited with V_s = 75 V. The other was a 4 μm thick YDC layer followed by a 1.5 μm thick YSZ layer (4YDC/1.5YSZ) deposited with V_s = 60 V. V_s = 30 to 60 V was used during YDC deposition. Annealing was carried out at 600°C for 4 h after the YDC layer deposition, and at 750°C for 4 h after the YSZ deposition. The highest temperature used in this study was 750°C, such that any interdiffusion between YDC and YSZ, which could lead to reduced ionic conductivity and electronic conduction,[19] was minimized. The anodes consisted of 0.2 μm thick porous YDC layers, deposited first to enhance anode performance, and 2 μm thick porous Ni-YSZ layers.[17] The cell test apparatus was similar to that described previously.[18] Cell tests were made in air and H_2-Ar fuel mixtures that had been passed through a 20°C water bubbler.

* Electrochemical Society Active Member.